



Heavy baryon decays into light meson and dark baryon within LCSR

Yu-Ji Shi^{1,2,a}, Ye Xing^{3,b}, Zhi-Peng Xing^{4,c}

¹ School of Physics, East China University of Science and Technology, Shanghai 200237, China

² Shanghai Key Laboratory of Particle Physics and Cosmology, School of Physics and Astronomy, Shanghai Jiao Tong University, Shanghai 200240, China

³ School of Materials Science and Physics, China University of Mining and Technology, Xuzhou 221116, China

⁴ Department of Physics and Institute of Theoretical Physics, Nanjing Normal University, Nanjing 210023, Jiangsu, China

Received: 30 January 2024 / Accepted: 10 March 2024 / Published online: 23 March 2024
© The Author(s) 2024

Abstract We studied the decays of Heavy baryon into a pseudoscalar meson and a dark baryon in the recently developed B -Mesogenesis scenario, where the two types of effective Lagrangians proposed by the scenario are both considered. The decay amplitudes of Λ_b^0 are calculated by light-cone sum rules using its light-cone distribution amplitudes. The decay amplitudes of $\Xi_b^{0,\pm}$ are related with those of Λ_b^0 through a flavor SU(3) analysis. The uncertainties of threshold parameter and the Borel parameter are both considered in the numerical calculation. The values of effective coupling constants in the B -Mesogenesis are taken as their upper limits that obtained from our previous study on the inclusive decay. The upper limits of the decay branching fractions are presented as functions of the dark baryon mass.

1 Introduction

The Standard Model of particle physics and cosmology have been proven to be successful in describing the physics of the most microscopic and macroscopic worlds. However, there is inconsistency between these two models, where two of the most confusing problems are the existence of dark matter (DM) and the asymmetry of matter and anti-matter. Nowadays, a number of mechanisms aiming to solve this puzzle have been proposed according to the Sakharov conditions for the baryogenesis [1]. One of the disadvantages among these mechanisms is the existence of high energy scales and extremely massive particles, which make them difficult to

be tested in experiments. Recently, a new mechanism called B -Mesogenesis is proposed by Refs. [2–6], which aims to explain both the relic dark matter abundance and the baryon asymmetry without introducing high energy scales. The B -Mesogenesis is testable at hadron colliders and B -factories [3, 7], and also indirectly testable at the Kaon and Hyperon factories [8, 9]. Recently, the Belle-II collaboration and the LHCb collaboration have started to search for the decays of B mesons with energy missing according to the B -Mesogenesis [10, 11].

The B -Mesogenesis proposes a new mechanism for Baryogenesis and DM production. In this model, during a late era in the history of the early universe, a certain heavy scalar particle Φ decays into b, \bar{b} quarks, which then form charged and neutral B -mesons after the universe cool down. After that, the neutral mesons B^0, \bar{B}^0 quickly undergo CP violating oscillations, and the remained mesons continue to decay into a dark sector baryon ψ with baryon number -1 and visible hadron states with baryon number $+1$. As a result, the asymmetry of the baryon and anti-baryon number from the CP violation during $B^0 - \bar{B}^0$ oscillations is induced but without violating the total baryon number. Recently, there are a number of theoretical studies on the B meson decays in the B -Mesogenesis. The exclusive decay $B \rightarrow p\psi$ was firstly studied by Ref. [12] using leading twist light-cone sum rules (LCSR) calculation, and a higher twist contribution are calculated in Ref. [13]. A more complete study on B meson decays into an octet baryon or a charmed anti-triplet baryon plus ψ was given in Ref. [14]. In addition, a similar exclusive decay of B meson into a baryon plus missing energy are studied by Ref. [15] for probing the lightest neutralino. Besides the exclusive decays, previously we studied the semi-inclusive decay of $B \rightarrow X_{u/c,d/s}\psi$ using heavy

^a e-mail: shiyuji@ecust.edu.cn (corresponding author)

^b e-mail: xingye_guang@cumt.edu.cn

^c e-mail: zpxing@sjtu.edu.cn

quark expansion (HQE), where $X_{u/c,d/s}$ denotes any possible hadron states containing u/c and d/s quarks with unit baryon number [16]. Using the experimental upper limits on the branching fractions of $B \rightarrow X_{u/c,d/s}\psi$ from the ALEPH experiment [17–19], we predicted the upper limits on the coupling constants in the B -Mesogenesis.

Up to now, the studies on the B -Mesogenesis mainly focus on the B decays. However, apart from the generous production of B meson in the LHCb and Belle experiments, Λ_b^0 is the most baryons that can be produced experimentally. In the B -Mesogenesis model, Λ_b^0 can also undergo baryon number violated decays such as $\Lambda_b \rightarrow M\psi$, where M is a neutral pseudoscalar meson including π^0, K^0, \bar{D}^0 . Compared with $B \rightarrow p/n\psi$, the phase space of $\Lambda_b^0 \rightarrow M\psi$ is larger, which can amplify the decay width to a certain extent so that offer more possibility for observing such decays in the experiments. In this work, we will perform a theoretical study on the $\Lambda_b^0 \rightarrow M\psi$ decays. The decay amplitude will be calculated by LCSR with the use of the light-cone distribution amplitudes (LCDAs) of Λ_b^0 . One disadvantage of $\Lambda_b^0 \rightarrow M\psi$ is that since the neutral final pseudoscalar meson makes it difficult to be detected. In contrast, the charged decay $\Xi_b^\pm \rightarrow M\psi$ should be a more ideal channel for experimental searching. In the flavor SU(3) symmetry limit, the decay amplitudes of these decay channels are related with each other. The SU(3) symmetry analysis is a powerful tools frequently used in heavy hadron decays [20–26], where it is generally be performed in two different frameworks: the topological diagram amplitude (TDA) and the irreducible representation amplitude (IRA) methods. These two methods have been proven to be equivalent in Refs. [23, 25, 27–30]. In this work, we will choose IRA method to obtain the relations between the decay amplitudes of $\Xi_b^\pm \rightarrow M\psi$ and those of $\Lambda_b^0 \rightarrow M\psi$, and use them to predict the decay branching fractions of $\Xi_b^\pm \rightarrow M\psi$.

This article is organized as follows: Sect. 2 introduces the B -Mesogenesis scenario proposed by Refs. [2–4]. Section 3 present a detailed LCSR calculation for the $\Lambda_b^0 \rightarrow M\psi$ decays. Section 4 present a SU(3) analysis on the decay amplitudes, which relates $\Xi_b^\pm \rightarrow M\psi$ to $\Lambda_b^0 \rightarrow M\psi$. Section 5 present numerical calculations on the decay amplitudes and branching fractions. Section 6 is a summary of this work.

2 The B -mesogenesis scenario

This section gives a brief introduction to the B -Mesogenesis scenario [2–4], which aims to simultaneously explain the baryon asymmetry and the existence of dark matter in our Universe. In the B -Mesogenesis scenario, the b quark is possible to decay into two light quarks and a dark baryon ψ . The total baryon number in such decay process is conserved, however, due to the invisible ψ the visible decay products exhibit baryon number non-conserving phenomenon. As pro-

posed by Refs. [2, 3], this kind of baryon number violating decays can emerge from the following two types of effective Lagrangians:

$$\begin{aligned} \mathcal{L}_{\text{eff}}^I &= -y_{ub}\epsilon_{ijk}Y^{*i}\bar{u}_R^j b_R^{c,k} - y_{cb}\epsilon_{ijk}Y^{*i}\bar{c}_R^j b_R^{c,k} \\ &\quad - y_{\psi d}Y_i\bar{\psi}d_R^{c,i} - y_{\psi s}Y_i\bar{\psi}s_R^{c,i} + \text{h.c.}, \\ \mathcal{L}_{\text{eff}}^{II} &= -y_{ud}\epsilon_{ijk}Y^{*i}\bar{u}_R^j d_R^{c,k} - y_{us}\epsilon_{ijk}Y^{*i}\bar{u}_R^j s_R^{c,k} \\ &\quad - y_{cd}\epsilon_{ijk}Y^{*i}\bar{c}_R^j d_R^{c,k} - y_{cs}\epsilon_{ijk}Y^{*i}\bar{c}_R^j s_R^{c,k} \\ &\quad - y_{\psi b}Y_i\bar{\psi}b_R^{c,i} + \text{h.c.}, \end{aligned} \tag{1}$$

which correspond to the type-I and II models in the B -Mesogenesis, respectively. All the quark fields are taken as right handed, the superscript c indicates charge conjugate and the y s are unknown coupling constants. Y is a charged color triplet scalar with $Q_Y = -1/3$, which is assumed to have large mass M_Y . In the Type-I model the b quark couples with u, c quarks, the dark anti-baryon ψ couples with d, s quarks. In the Type-II model, the situations of the b and d, s quarks are interchanged. In fact, as proposed by Ref. [3], there should be a third type of effective Lagrangian with $Q_Y = 2/3$ in B -Mesogenesis, which reads as

$$\begin{aligned} \mathcal{L}_{\text{eff}}^{III} &= -y_{bd}\epsilon_{ijk}Y^{*i}\bar{b}_R^j d_R^{c,k} - y_{bs}\epsilon_{ijk}Y^{*i}\bar{b}_R^j s_R^{c,k} \\ &\quad - y_{\psi u}Y_i\bar{\psi}u_R^{c,i} - y_{\psi c}Y_i\bar{\psi}c_R^{c,i} + \text{h.c.} \end{aligned} \tag{2}$$

In this work, we will only consider the case of $Q_Y = -1/3$ to be consistent with the studies of exclusive B meson decay in B -Mesogenesis [12, 14].

Integrating out the heavy boson Y in Eq. (1), one can obtain the effective Hamiltonian for the two types of models as:

$$\begin{aligned} \mathcal{H}_{\text{eff}}^{I,uq} &= -\frac{y_{ub}y_{\psi q}}{M_Y^2}i\epsilon_{ijk}(\bar{\psi}q_R^{c,i})(\bar{u}_R^j b_R^{c,k}) + \text{h.c.} \\ &= -G_{(uq)}^I \bar{O}_{(uq)}^I \psi^c + \text{h.c.}, \\ \mathcal{H}_{\text{eff}}^{II,uq} &= -\frac{y_{\psi b}y_{uq}}{M_Y^2}i\epsilon_{ijk}(\bar{\psi}b_R^{c,i})(\bar{u}_R^j q_R^{c,k}) + \text{h.c.} \\ &= -G_{(uq)}^{II} \bar{O}_{(uq)}^{II} \psi^c + \text{h.c.}, \end{aligned} \tag{3}$$

where for simplicity, $q = s, d$ and we use u to denote the u or c quarks simultaneously. The effective coupling constant and the effective operators in the two models are defined as

$$\begin{aligned} G_{(uq)}^I &= \frac{y_{ub}y_{\psi q}}{M_Y^2}, & \mathcal{O}_{(uq)}^I &= -i\epsilon_{ijk}(u^{iT} C P_R b^j) P_R q^k, \\ G_{(uq)}^{II} &= \frac{y_{\psi b}y_{uq}}{M_Y^2}, & \mathcal{O}_{(uq)}^{II} &= -i\epsilon_{ijk}(u^{iT} C P_R q^j) P_R b^k, \end{aligned} \tag{4}$$

where $P_R = (1 + \gamma_5)/2$ and C is the charge conjugate matrix. The baryon number violated decays $\Lambda_b \rightarrow \pi\psi, \Lambda_b \rightarrow K\psi$

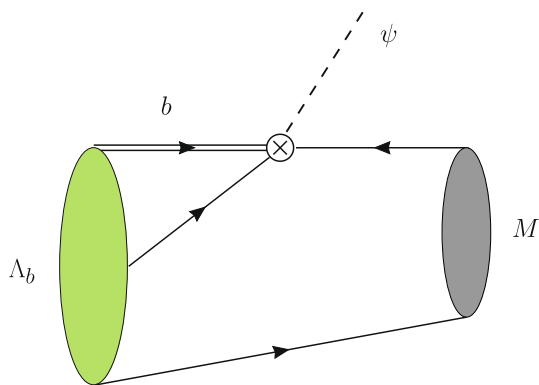


Fig. 1 The Feynman diagram of the $\Lambda_b \rightarrow M\psi$ decays. The green and gray bubbles denote the Λ_b and pseudoscalar M , respectively, and the white crossed dot denotes the $\mathcal{O}_{(uq)}$ vertex

and $\Lambda_b \rightarrow D\psi$ are induced by $\mathcal{H}_{\text{eff}}^{I,ud}$, $\mathcal{H}_{\text{eff}}^{I,us}$ and $\mathcal{H}_{\text{eff}}^{I,cd}$ respectively.

3 $\Lambda_b \rightarrow M\psi$ decays in LCSR

3.1 Hadron level calculation

In this section, we perform a LCSR calculation on the $\Lambda_b \rightarrow M\psi$ decays as shown in Fig. 1. The green and gray bubbles denote the Λ_b and pseudoscalar M , respectively, and the white crossed dot denotes the $\mathcal{O}_{(uq)}$ vertex. Using the effective Hamiltonians given in Eq. (3), one can express the decay amplitude as

$$i\mathcal{M} = -G_{(uq)} \bar{u}_\psi^c(q, s_\psi) \langle M(p') | \mathcal{O}_{(uq)}(0) | \Lambda_b(p, s_\Lambda) \rangle, \quad (5)$$

where u_ψ is the spinor of dark baryon, with momentum $q = p - p'$. The transition matrix element on the right hand side above can be parameterized by two form factors:

$$\begin{aligned} &\langle M(p') | \mathcal{O}_{(uq)}(0) | \Lambda_b(p, s_\Lambda) \rangle \\ &= P_R \left[F_1(q^2) + \frac{q}{m_{\Lambda_b}} F_2(q^2) \right] u_{\Lambda_b}(p, s_\Lambda). \end{aligned} \quad (6)$$

In the framework of LCSR, the calculation of the transition matrix element given above starts from the following two-point correlation function

$$\begin{aligned} &\Pi(p, q) \\ &= i \int d^4x e^{ip \cdot x} q^\mu \langle 0 | T \{ j_\mu^M(x) \mathcal{O}_{(uq)}(0) \} | \Lambda_b(p + q) \rangle, \end{aligned} \quad (7)$$

where j_μ^M denotes the interpolation current for the final meson, which reads as

$$\begin{aligned} j_\mu^\pi &= \frac{1}{\sqrt{2}} (\bar{u} \gamma_\mu \gamma_5 u - \bar{d} \gamma_\mu \gamma_5 d), & j_\mu^K &= \bar{s} \gamma_\mu \gamma_5 d, \\ \text{and } j_\mu^D &= \bar{c} \gamma_\mu \gamma_5 d \end{aligned} \quad (8)$$

for the final states: $M = \pi^0, K^0$ and D^0 respectively. In LCSR, the correlation function defined in Eq. (7) will be calculated both at the hadron and quark-gluon level. The one at hadron level can be expressed by the form factors defined in Eq. (6). On the other hand, the one at quark-gluon level will be calculated explicitly in QCD, with the light-cone distribution amplitudes (LCDAs) of Λ_b taken as non-perturbative inputs. Matching of the correlation function at these two levels enables us to extract the transition form factors.

At the hadron level, one inserts a complete set of states with the same quantum number of M between the $j_\mu^M(q^2)$ current and $\mathcal{O}_{(uq)}(0)$. The correlation function becomes

$$\begin{aligned} \Pi^H(p, q) &= \frac{if_M}{m_M^2 - p^2} (p \cdot q) P_R \\ &\times \left[F_1(q^2) + \frac{q}{m_{\Lambda_b}} F_2(q^2) \right] u_{\Lambda_b}(p + q) \\ &+ \int_{s_{\text{th}}}^\infty ds \frac{\rho^H(s, q)}{s - p^2}, \end{aligned} \quad (9)$$

where the meson decay constant is defined as: $\langle 0 | j_\mu^M(0) | M(p) \rangle = if_M p_\mu$. Here only the pole contribution from M is expressed explicitly, while the contribution from excited state and continuous spectrum above threshold s_{th} are captured in the integration of $\rho^H(s, q)$, which will be suppressed by Borel transformation. Note that in the expression: $p \cdot q = (1/2)(m_{\Lambda_b}^2 - q^2 - m_M^2) + (1/2)(m_M^2 - p^2)$, the second term will cancel the denominator of the pole contribution in Eq. (9), so that the terms proportional to it will vanish under the Borel transformation on p^2 . As a result, the Borel transformed correlation function becomes

$$\begin{aligned} \mathcal{B}\{\Pi^H\}(p, q) &= \frac{i}{2} f_M (m_{\Lambda_b}^2 - q^2 - m_M^2) e^{-m_M^2/T^2} P_R \\ &\times \left[F_1(q^2) + \frac{q}{m_{\Lambda_b}} F_2(q^2) \right] u_{\Lambda_b}(p + q) \\ &+ \int_{s_{\text{th}}}^\infty ds e^{-s/T^2} \rho^H(s, q), \end{aligned} \quad (10)$$

where T is the Borel parameter. Now the contributions from excited state and continuous spectrum are suppressed by the exponential term e^{-s/T^2} . Next, the same correlation function will be calculated at the quark-gluon level, where the result

can be generally written as a dispersion integration form

$$\Pi^{QCD}(p, q) = \frac{1}{\pi} \int_{s_m}^{\infty} ds \frac{\text{Im}\Pi^{QCD}(s, q)}{s - p^2}, \tag{11}$$

with s_m being the quark level threshold. From the assumption of quark-hadron duality, the last term of Eq. (9), denoting the excited state and continuous spectrum at hadron level, is equivalent with the spectrum integration above s_{th} at quark-gluon level. After the Borel transformation and subtracting the continuous spectrum contribution, we arrive at the sum rules equation:

$$\begin{aligned} \mathcal{B}\{\Pi^H\}(p, q)_{\text{pole}} &= \mathcal{B}\{\Pi^{QCD}\}(p, q) \\ &= \frac{1}{\pi} \int_{s_m}^{s_{th}} ds e^{-s/T^2} \text{Im}\Pi^{QCD}(s, q). \end{aligned} \tag{12}$$

Thus the form factors $F_{1,2}$ can be extracted through this equation as long as the imaginary part of Π^{QCD} is obtained.

3.2 Quark-gluon level calculation

Now we perform an quark-gluon level calculation for the correlation function defined in Eq. (7). Here we take the type-I model and the case of $M = \bar{D}^0$ as an example to illustrate the calculation. Using the quark level expression of j_{μ}^D given in Eq. (8), one can write the correlation function as

$$\begin{aligned} [\Pi_{\Lambda_b \rightarrow D}^{QCD}(p, q)]_{\kappa} &= -\epsilon_{ijk} \int d^4x e^{ip \cdot x} \\ &\times [P_R C S_c(0, x) q \gamma_5]_{\gamma\alpha} (P_R)_{\kappa\beta} \\ &\times \langle 0 | u_{\alpha}^i(q^2) d_{\beta}^j(0) b_{\gamma}^k(0) | \Lambda_b(p + q) \rangle, \end{aligned} \tag{13}$$

where S_c is the charm quark propagator. Note that the correlation function has a structure of spinor and the corresponding spinor index is denoted as κ . α, β, γ are also spinor indexes, while i, j, k denote color indexes. The non-local three quark matrix element above is expressed by the Λ_b LCDAs, which are defined as [31,32]

$$\begin{aligned} \epsilon_{ijk} \langle 0 | u_{\alpha}^i(x_1) d_{\beta}^j(x_2) b_{\gamma}^k(0) | \Lambda_b(v) \rangle &= \frac{1}{8} f_{\Lambda_b}^{(2)} \Psi_2(t_1, t_2) (\not{n} \gamma_5 C)_{\alpha\beta} u_{\Lambda_b\gamma}(v) \\ &+ \frac{1}{4} f_{\Lambda_b}^{(1)} \Psi_3^s(t_1, t_2) (\gamma_5 C)_{\alpha\beta} u_{\Lambda_b\gamma}(v) \\ &- \frac{1}{8} f_{\Lambda_b}^{(1)} \Psi_3^{\sigma}(t_1, t_2) (i\sigma_{\bar{n}n} \gamma_5 C)_{\alpha\beta} u_{\Lambda_b\gamma}(v) \\ &+ \frac{1}{8} f_{\Lambda_b}^{(2)} \Psi_4(t_1, t_2) (\not{n} \gamma_5 C)_{\alpha\beta} u_{\Lambda_b\gamma}(v), \end{aligned} \tag{14}$$

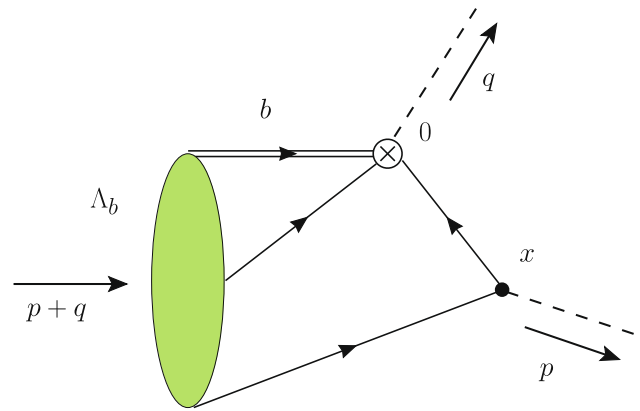


Fig. 2 The Feynman diagram of the the correlation function defined in Eq. (7). The green bubble denotes the Λ_b LCDAs, the white crossed and the black dots denote the $\mathcal{O}_{(uq)}(x)$ and the $j_{\mu}^M(0)$ vertices, respectively

where $\sigma_{\bar{n}n} = \sigma_{\mu\nu} \bar{n}^{\mu} n^{\nu}$ and $x_1 = t_1 n, x_2 = t_2 n$ are on the light cone. Inversely, the light cone vectors n, \bar{n} can be expressed by the coordinates as

$$n_{\mu} = \frac{x_{\mu}}{v \cdot x}, \quad \bar{n}_{\mu} = 2v_{\mu} - \frac{x_{\mu}}{v \cdot x}.$$

At the quark-gluon level, the corresponding diagram for the correlation function defined in Eq. (7) is shown in Fig. 2. The green bubble denotes the Λ_b LCDAs, the white crossed and the black dots denote the $\mathcal{O}_{(uq)}(x)$ at and the $j_{\mu}^M(0)$ vertices, respectively.

The $\Psi_2, \Psi_3^s, \Psi_3^{\sigma}, \Psi_4$ in Eq. (14) are the LCDAs with different twists. In the momentum space, the LCDAs can be characterized by the total momentum ω of the two light quarks in Λ_b , and the momentum fraction u of one light quark:

$$\Psi_i(t_1, t_2) = \int_0^{\infty} \omega d\omega \int_0^1 du e^{-i\omega(t_1 u + t_2 \bar{u})} \psi_i(\omega, u), \tag{15}$$

with $\bar{u} = 1 - u$, and [31]

$$\begin{aligned} \psi_2(\omega, u) &= \omega^2 u(1-u) \left[\frac{1}{\epsilon_0^4} e^{-\omega/\epsilon_0} + a_2 C_2^{3/2}(2u-1) \right. \\ &\quad \left. \times \frac{1}{\epsilon_1^4} e^{-\omega/\epsilon_1} \right], \\ \psi_3^s(\omega, u) &= \frac{\omega}{2\epsilon_3^3} e^{-\omega/\epsilon_3}, \\ \psi_3^{\sigma}(\omega, u) &= \frac{\omega}{2\epsilon_3^3} (2u-1) e^{-\omega/\epsilon_3}, \\ \psi_4(\omega, u) &= 5\mathcal{N}^{-1} \int_{\omega/2}^{s_0^{\Lambda_b}} ds e^{-s/\tau} (s - \omega/2)^3, \end{aligned} \tag{16}$$

where $C_2^{3/2}(2u-1)$ is the Gegenbauer polynomial, and the normalization factor \mathcal{N} in $\tilde{\psi}_4(\omega, u)$ reads as $\mathcal{N} = \int_0^{s_0^{\Lambda_b}} ds s^5 e^{-s/\tau}$. These four LCDAs are calculated by QCD

sum rules in Ref. [31], with τ being the Borel parameter for the sum rules calculation. All the parameters involved in the LCDAs are $\epsilon_0 = 200^{+130}_{-60}$ MeV, $\epsilon_1 = 650^{+650}_{-300}$ MeV, $\epsilon_3 = 230$ MeV, $a_2 = 0.333^{+0.250}_{-0.333}$, $s_0^{\Lambda_b} = 1.2$ GeV and $\tau = 0.4\text{--}0.8$ GeV. [31].

Using the LCDAs defined in Eq. (14), and the free charm quark propagator, one can express the correlation function as a convolution of the perturbative part and the LCDAs. Firstly, the twist-3 s contribution can be straightforwardly written as

$$\begin{aligned} \Pi_{\Lambda_b \rightarrow D}^{QCD(3s)}(p, q) &= \frac{i}{4} f_{\Lambda_b}^{(1)} \int_0^{2s_0^{\Lambda_b}} d\omega \omega \int_0^1 du \psi_{3s}(\omega, u) \\ &\times \frac{1}{(u\omega v - p)^2 - m_c^2} P_R \not{q} (u\omega \not{p} - \not{p}) u_{\Lambda_b}(v). \end{aligned} \tag{17}$$

To extract the imaginary part of correlation function, one has to calculate its discontinuity across the complex plane of p^2 . The denominator can be rewritten as

$$\begin{aligned} (u\omega v - p)^2 - m_c^2 &= \left(1 - \frac{u\omega}{m_{\Lambda_b}}\right) (p^2 - \Sigma_c), \\ \Sigma_c &= \frac{1}{m_{\Lambda_b} - u\omega} \left[u\omega (m_{\Lambda_b}^2 - q^2) + m_{\Lambda_b} (m_c^2 - u^2\omega^2) \right]. \end{aligned} \tag{18}$$

Now the imaginary part comes from the term

$$\text{Im} \left[\frac{1}{(u\omega v - p)^2 - m_c^2} \right] = \frac{1}{2i} (-2\pi i) \frac{m_{\Lambda_b}}{m_{\Lambda_b} - u\omega} \delta(s - \Sigma_c), \tag{19}$$

where $s = p^2$. Expressing $\Pi_{\Lambda_b \rightarrow D}^{QCD(3s)}$ as a dispersion integration in $s_m < s < s_{th}$, performing the Borel transformation, and integrating out s by the delta function in Eq. (19), one arrives at

$$\begin{aligned} \mathcal{B}\{\Pi_{\Lambda_b \rightarrow D}^{QCD(3s)}\}(T, q) &= \frac{i}{4} f_{\Lambda_b}^{(1)} \int_0^{2s_0^{\Lambda_b}} d\omega \\ &\times \int_0^1 du \theta(\Sigma_c - s_m) \theta(s_{th} - \Sigma_c) e^{-\Sigma_c/T^2} \\ &\times \psi_{3s}(\omega, u) P_R \left[m_{\Lambda_b} \omega \not{q} - \frac{m_{\Lambda_b} \omega}{m_{\Lambda_b} - u\omega} q^2 \right]. \end{aligned} \tag{20}$$

The calculation for the twist-3 σ contribution is more involved. The corresponding correlation function can be firstly written as

$$\begin{aligned} \Pi_{\Lambda_b \rightarrow D}^{QCD(3\sigma)}(p, q) &= -\frac{i}{4} f_{\Lambda_b}^{(1)} \int d^4x e^{ip \cdot x} \int_0^{2s_0^{\Lambda_b}} d\omega \omega \\ &\times \int_0^1 du e^{-iu\omega v \cdot x} \int \frac{d^4k}{(2\pi)^4} e^{ik \cdot x} \end{aligned}$$

$$\times \psi_{3s}(\omega, u) P_R (1 - \not{u} \not{p}) \not{q} \frac{1}{\not{k}} u_{\Lambda_b}(v), \tag{21}$$

where the 4-velocity of Λ_b is $m_{\Lambda_b} v = p + q$. It can be found that the term containing no \not{u} above has almost the same form as that of $\Pi_{\Lambda_b \rightarrow D}^{QCD(3s)}$. The corresponding contribution to the Borel transformed $\Pi_{\Lambda_b \rightarrow D}^{QCD(3\sigma)}$ is

$$\begin{aligned} \mathcal{B}\{\Pi_{\Lambda_b \rightarrow D}^{QCD(3\sigma(1))}\}(T, q) &= -\frac{i}{4} f_{\Lambda_b}^{(1)} \int_0^{2s_0^{\Lambda_b}} d\omega \\ &\times \int_0^1 du e^{-\Sigma_c/T^2} \theta(\Sigma_c - s_m) \theta(s_{th} - \Sigma_c) \\ &\times \psi_{3\sigma}(\omega, u) P_R \left[m_{\Lambda_b} \omega \not{q} - \frac{m_{\Lambda_b} \omega}{m_{\Lambda_b} - u\omega} q^2 \right]. \end{aligned} \tag{22}$$

Next we consider the term proportional to \not{u} in Eq. (21). Note that $n_\mu = x_\mu/v \cdot x$, to eliminate the $1/v \cdot x$ one can define modified LCDAs as

$$\bar{\psi}_i(\omega, u) = \int_0^\omega d\tau \tau \psi_i(\tau, u), \tag{23}$$

with $i = 2, 3s, 3\sigma, 4$. Thus the $1/v \cdot x$ can be eliminated through integration by part:

$$\begin{aligned} &\int_0^{2s_0^{\Lambda_b}} d\omega \omega \psi_i(\omega, u) e^{-iu\omega v \cdot x} \frac{x_\mu}{v \cdot x} \\ &= iu \int_0^{2s_0^{\Lambda_b}} d\omega \bar{\psi}_i(\omega, u) e^{-iu\omega v \cdot x} x_\mu. \end{aligned} \tag{24}$$

Here the boundary term has been omitted since large ω in the exponential induces high frequency oscillation under the integration of x , which suppresses its contribution. The x_μ can be written as $-i\partial/\partial p^\mu$, and thus the \not{u} term in Eq. (21) contributes:

$$\begin{aligned} \Pi_{\Lambda_b \rightarrow D}^{QCD(3\sigma(n))}(p, q) &= \frac{i}{4} f_{\Lambda_b}^{(1)} \int_0^{2s_0^{\Lambda_b}} d\omega \omega \int_0^1 du \bar{\psi}_{3\sigma}(\omega, u) \\ &\times P_R \frac{\partial}{\partial p^\mu} \left[\frac{1}{(p - u\omega)^2 - m_c^2} \gamma^\mu \not{p} \not{q} (u\omega \not{p} - \not{p}) \right] u_{\Lambda_b}(v). \end{aligned} \tag{25}$$

After dispersion integration, performing the Borel transformation, and introducing auxiliary mass to lower the higher power of denominators: $1/(p^2 - \Sigma_c)^2 = (\partial/\partial M^2)[1/(p^2 - \Sigma_c - M^2)]|_{M^2=0}$, one obtains the \not{u} term contribution as

$$\begin{aligned} \mathcal{B}\{\Pi_{\Lambda_b \rightarrow D}^{QCD(3\sigma(n))}\}(T, q) &= -\frac{i}{2} f_{\Lambda_b}^{(1)} \frac{\partial}{\partial M^2} \int_0^{2s_0^{\Lambda_b}} d\omega \int_0^1 du u \bar{\psi}_{3\sigma}(\omega, u) \end{aligned}$$

$$\begin{aligned} &\theta[(\Sigma_c + M^2) - s_m]\theta[s_{th} - (M^2 + \Sigma_c)]e^{-(\Sigma_c+M^2)/T^2} \\ &\times P_R \left(\frac{m_{\Lambda_b}}{m_{\Lambda_b} - u\omega} \right)^2 \left[A(p^2, q^2) + (2v \cdot q)m_c^2 \right. \\ &\left. + B(p^2, q^2)\not{q} \right] u_{\Lambda_b}(v) \Big|_{M^2=0, p^2=\Sigma_c+M^2}, \end{aligned} \tag{26}$$

where

$$\begin{aligned} A(p^2, q^2) &= (2v \cdot q)(m_{\Lambda_b} - u\omega)(m_{\Lambda_b} + u\omega - 2v \cdot p) \\ &\quad - 2(m_{\Lambda_b} - v \cdot p)q^2, \\ B(p^2, q^2) &= q^2 - (m_{\Lambda_b} - u\omega)(m_{\Lambda_b} + u\omega - 2v \cdot p), \end{aligned} \tag{27}$$

and note that all the Lorentz invariants involved above should be expressed by p^2, q^2 as

$$\begin{aligned} v \cdot q &= \frac{1}{2m_{\Lambda_b}}(m_{\Lambda_b}^2 + q^2 - p^2), \\ v \cdot p &= \frac{1}{2m_{\Lambda_b}}(m_{\Lambda_b}^2 + p^2 - q^2), \\ p \cdot q &= \frac{1}{2}(m_{\Lambda_b}^2 - q^2 - p^2). \end{aligned} \tag{28}$$

The twist-2 and 4 contributions to the correlation function can be obtained similarly as that of twist-3. The corresponding Borel transformed correlation function is

$$\begin{aligned} &\mathcal{B}\{\Pi_{\Lambda_b \rightarrow D}^{QCD(2)+(4)}\}(p, q) \\ &= \frac{i}{4}m_c f_{\Lambda_b}^{(2)} \int_0^{2s_0^{\Lambda_b}} d\omega \int_0^1 du u e^{-\Sigma_c/T^2} \theta(\Sigma_c - s_m) \theta(s_{th} - \Sigma_c) \\ &\quad \times \psi_2(\omega, u) \left(\frac{\omega m_{\Lambda_b}}{m_{\Lambda_b} - u\omega} \right) P_R [2v \cdot q - \not{q}] u_{\Lambda_b}(v) \Big|_{M^2=0} \\ &\quad + \frac{i}{4}m_c f_{\Lambda_b}^{(2)} \frac{\partial}{\partial M^2} \int_0^{2s_0^{\Lambda_b}} d\omega \int_0^1 du u e^{-(\Sigma_c+M^2)/T^2} \theta \\ &\quad \times (\Sigma_c + M^2 - s_m) \theta(s_{th} - M^2 - \Sigma_c) (\bar{\psi}_2 - \bar{\psi}_4)(\omega, u) \\ &\quad \times \left(\frac{m_{\Lambda_b}}{m_{\Lambda_b} - u\omega} \right)^2 P_R [2p \cdot q + q^2 - 2u\omega v \cdot q - (m_{\Lambda_b} \\ &\quad - u\omega)\not{q}] u_{\Lambda_b}(v) \Big|_{M^2=0, p^2=\Sigma_c+M^2}. \end{aligned} \tag{29}$$

It can be found that here the twist-2 and 4 contributions are proportional to m_c . In the case of $\Lambda_b \rightarrow \pi, K + \psi$ decays, the twist-2 and 4 contributions are proportional to $m_u = m_d = 0$ and thus vanish. For the $\Lambda_b \rightarrow \pi, K + \psi$ decays in the type-I model, the calculation of the correlation function in Eq. (7) is almost the same, which can be found in the Appendix A.

Generally, as Eq. (10) shows, the correlation function has two independent spinor structures: 1 and \not{q} . In the type-I model both of them exists in the correlation function. However, it can be found that the \not{q} term is absent in the type-

II model. As a result, only F_1 contributes to the $\Lambda_b^0 \rightarrow \pi^0, K^0, \bar{D}^0 + \psi$ decays, while F_2 vanishes up to the twist-3 LCDA contributions. On the other hand, in the type-II model the $\Lambda_b^0 \rightarrow \pi^0 + \psi$ decay is forbidden due to the flavor SU(3) limit, which will be discussed in the next section. The corresponding analytical results in the type-II models are given in the Appendix B.

4 SU(3) analysis

In the above study we have only focused on the decay processes $\Lambda_b^0 \rightarrow \pi^0, K^0, \bar{D} + \psi$, while the various decay channels $\Xi_b^{0,-} \rightarrow \pi^{0,-}, K^{0,-} + \psi$ and $\Lambda_b^0, \Xi_b^0 \rightarrow \eta + \psi$ have not been considered. In principle, the amplitudes of these missed processes can also be calculated as soon as the LCDAs of Ξ_b or η are known, which have not been studied as well as the LCDAs of Λ_b . However, with the use of flavor SU(3) symmetry, one can still able to predict the decay widths of these missed channels as long as the decay widths of $\Lambda_b^0 \rightarrow \pi^0, K^0 + \psi$ are known.

As shown in Eq. (3), the effective Hamiltonian: $-G_{uq} \mathcal{O}(uq)$ contains two light quark fields u, d or u, s . In the flavor SU(3) representation, this Hamiltonian can be represented by a rank-two tensor H_{ij} , where i, j are the flavor indexes. Its non-vanishing components are $H_{12} = G_{ud}$ and $H_{13} = G_{us}$ for $b \rightarrow u, d$ and $b \rightarrow u, s$ transitions, respectively. Note that H_{ij} is reducible so that can be further be reduced into three SU(3) irreducible representations: a symmetric and traceless tensor $\bar{S}_{[ij]}$, an anti-symmetry tensor $T_{[ij]}$ and a trace term $I\delta_{ij}$:

$$H_{ij} = \bar{S}_{[ij]} + T_{[ij]} + I\delta_{ij}, \tag{30}$$

where

$$\bar{S}_{[ij]} = \frac{1}{2}H_{ij} + \frac{1}{2}H_{ji} - \frac{1}{3}\delta_{ij}H_{kk}, \quad T_{[ij]} = \frac{1}{2}H_{ij} - \frac{1}{2}H_{ji}. \tag{31}$$

The non-vanishing components are $\bar{S}_{12} = \bar{S}_{21} = \frac{1}{2}, T_{12} = -T_{21} = \frac{1}{2}$ for $b \rightarrow u, d$, and $\bar{S}_{13} = \bar{S}_{31} = \frac{1}{2}, T_{13} = -T_{31} = \frac{1}{2}$ for $b \rightarrow u, s$. It should be mentioned that in the type-II model, as shown by Eq. (4) the two light flavors are anti-symmetrized, so that \bar{S}_{ij} vanishes in this case.

On the other hand, the initial anti-triplet baryons $T_{\mathbf{\bar{3}}}$ and the final light mesons M can also be expressed by SU(3) irreducible representations as

$$(T_{\mathbf{\bar{3}}}^{ij}) = \begin{pmatrix} 0 & \Lambda_b^0 & \Xi_b^0 \\ -\Lambda_b^0 & 0 & \Xi_b^- \\ -\Xi_b^0 & -\Xi_b^- & 0 \end{pmatrix}_{ij},$$

Table 1 Decay amplitudes of anti-triplet bottom baryon decays into a light meson and dark baryon from Eq. (33), where the left and right columns correspond to $b \rightarrow d$ and $b \rightarrow s$ transitions, respectively

Channel	Amplitude	Channel	Amplitude
$\Lambda_b^0 \rightarrow \pi^0 \psi$	$\sqrt{2}s_1 G_{ud}$	$\Lambda_b^0 \rightarrow K^0 \psi$	$-(s_1 + t_1)G_{us}$
$\Xi_b^0 \rightarrow \bar{K}^0 \psi$	$-(s_1 + t_1)G_{ud}$	$\Xi_b^0 \rightarrow \pi^0 \psi$	$\frac{1}{\sqrt{2}}(s_1 - t_1)G_{us}$
$\Xi_b^- \rightarrow K^- \psi$	$-(s_1 - t_1)G_{ud}$	$\Xi_b^- \rightarrow \pi^- \psi$	$(s_1 - t_1)G_{us}$
$\Lambda_b^0 \rightarrow \eta \psi$	$-\sqrt{\frac{2}{3}}t_1 G_{ud}$	$\Xi_b^0 \rightarrow \eta \psi$	$(\frac{1}{\sqrt{6}}t_1 - \sqrt{\frac{3}{2}}s_1)G_{us}$

$$M_j^i = \begin{pmatrix} \frac{\pi^0}{\sqrt{2}} + \frac{\eta}{\sqrt{6}} & \pi^+ & K^+ \\ \pi^- & -\frac{\pi^0}{\sqrt{2}} + \frac{\eta}{\sqrt{6}} & K^0 \\ K^- & \bar{K}^0 & -\frac{2\eta}{\sqrt{6}} \end{pmatrix}_{ij}. \tag{32}$$

Using $T_{b\bar{3}}, M_j^i, \bar{S}_{ij}$ and T_{ij} , one can construct SU(3) invariant amplitude as

$$\mathcal{A} = s_1 T_{b\bar{3}}^{ij} \bar{S}_{jk} (M^T)_i^k \psi + t_1 T_{b\bar{3}}^{ij} T_{jk} (M^T)_i^k \psi + t_2 T_{b\bar{3}}^{ij} T_{ij} (M^T)_k^k \psi. \tag{33}$$

Here we have not considered the color singlet η_1 in the construction of M_j^i , thus the third term above vanishes due to $M_k^k = 0$. The unknown amplitudes s_1, t_1, t_2 contain all the information about the strong interaction in the decays. All the decay amplitudes of anti-triplet bottom baryon decays into a light meson and dark baryon are listed in Table 1, where the left and right two columns correspond to $b \rightarrow d$ and $b \rightarrow s$ transitions.

Note that the amplitude of $\Lambda_b^0 \rightarrow \pi^0 + \psi$ is proportional to s_1 which is absent in the type-II model. Therefore, in the type-II model the $\Lambda_b^0 \rightarrow \pi^0 + \psi$ decay is forbidden, and we have $s_1 = 0$ in Table 1 so that the amplitudes of all the decay channels are proportional to t_1 . On the other hand, in the type-I model, using the decay amplitudes of $\Lambda_b^0 \rightarrow \pi^0 \psi$ and $\Lambda_b^0 \rightarrow K^0 \psi$ calculated in this work by LCSR, we can determine the fraction $\xi_{K/\pi} = t_1/s_1$ as

$$-\frac{1}{\sqrt{2}}(1 + \xi_{K/\pi})\lambda_{s/d} = \frac{\mathcal{A}(\Lambda_b^0 \rightarrow K^0 \psi)}{\mathcal{A}(\Lambda_b^0 \rightarrow \pi^0 \psi)}, \tag{34}$$

with $\lambda_{s/d} = G_{us}/G_{ud}$. This enables us to predict all the decay amplitudes listed in Table 1.

5 Numerical results

The hadron masses are taken as: $m_{\Lambda_b} = 5.62$ GeV, $m_\pi = 0.135$ GeV, $m_K = 0.498$ GeV and $m_D = 1.86$ GeV. The quark masses are taken as $m_u = m_d = 0$ and $m_c = 1.1$ GeV at $\mu = 3$ GeV [33]. $\tau = 0.6$ GeV is taken as the center

value in its range $\tau = 0.4 \sim 0.8$ GeV. The threshold parameters should be above the lowest state while nearly below the next lowest state. The next lowest states corresponding to π, D, K are $\pi(1300), K(1460), D(2550)$ [33] and s_{th} can be parameterized as

$$s_{th}^{\pi,K,D} = (1 - \lambda)m_{\pi,K,D}^2 + \lambda m_{\pi(1300),K(1460),D(2550)}^2, \tag{35}$$

where $\lambda = 0$ and $\lambda = 1$ correspond to the lowest and the next lowest states, respectively. In this work, to estimate the uncertainties from the threshold parameter, we choose the range $0.6 < \lambda < 1.0$ for error analysis in numerical calculations.

Now we have to exam the behavior of the form factors F_1, F_2 as functions of T^2 , and determine the choice of T^2 value. In principle, the physical results should be independent of the Borel parameters, and thus one has to find a T^2 region where the behavior of F_1, F_2 are almost stable. In Figs. 3 and 4, the form factors F_1, F_2 are plotted in a wide range of T^2 for the type-I and II models respectively, with $q^2 = 0$. It can be found that when T^2 is large, the form factors become stable and the curves are almost flat. On the other hand, in order to suppress the continuous spectrum contribution before quark-hadron duality, the T^2 cannot be too large according to the exponential term in Eq. (12). Quantitatively, this requirement can be expressed as

$$\xi(T^2) \equiv \frac{\int_{s_{th}}^\infty ds e^{-s/T^2} \text{Im}\Pi^{QCD}(s, q)}{\int_{s_m}^\infty ds e^{-s/T^2} \text{Im}\Pi^{QCD}(s, q)} < 50\%, \tag{36}$$

where the integrand is the same as that in Eq. (12). In the numerator, the integration in the range $s_{th} < s < \infty$ denotes the continuous spectrum contribution, while the integration in the denominator denotes the sum of pole and continuous spectrum contributions. It can be found that $\xi(T^2)$ increases with the increasing of T^2 , and thus Eq. (36) in principle determines the upper limit of T^2 . Actually, in the wide T^2 regions as shown in Figs. 3 and 4, the requirement $\xi(T^2) < 50\%$ has already been safely satisfied, and the maximum ξ in these regions are listed in Table 2.

Therefore, the upper limit values of T^2 can be safely chosen from the flat regions in Figs. 3 and 4 with a certain degree of arbitrariness, which has negligible impact on the error analysis. On the other hand, since in this work only the leading order QCD calculation is performed, one cannot determine the lower limits of T^2 by comparing the leading and next-to-leading order contributions. Therefore, here we choose the lower limits of T^2 in the region slightly below the stable region. Although choosing T^2 around unstable T^2 region may introduce more uncertainties on the result, this will make the phenomenological prediction more conservative for the new physics searching. Finally, we choose the

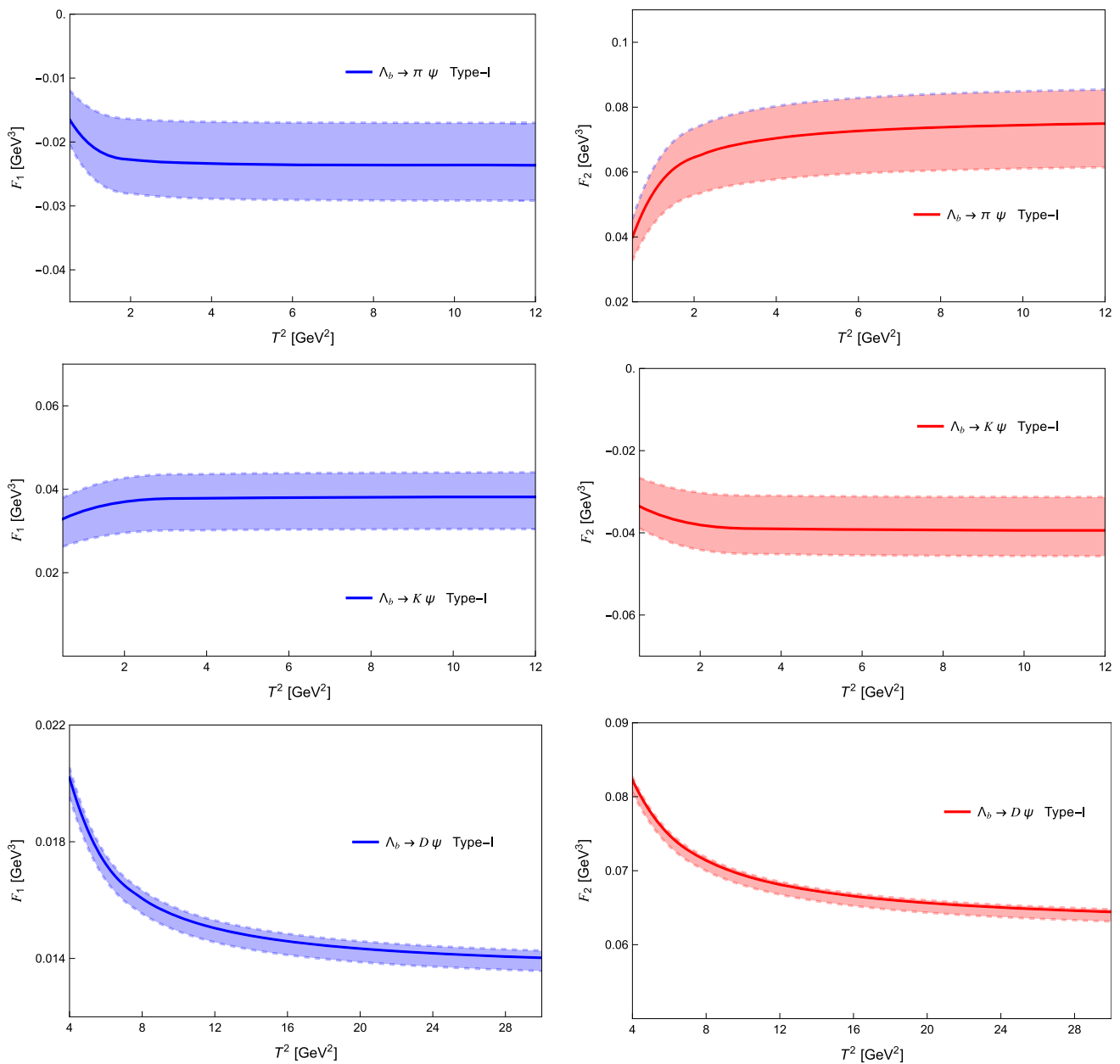


Fig. 3 The form factors F_1, F_2 as functions of T^2 in the type-I model, with $q^2 = 0$. The band width denotes the uncertainty of s_{th} : $0.6 < \lambda < 1.0$

ranges of T^2 as

$$\begin{aligned} \Lambda_b \rightarrow \pi \psi, K \psi : 4 \text{ GeV}^2 < T^2 < 12 \text{ GeV}^2, \\ \Lambda_b \rightarrow D \psi : 12 \text{ GeV}^2 < T^2 < 28 \text{ GeV}^2 \end{aligned} \quad (37)$$

for both the type-I and II models.

On the other hand, note that the $F_{1,2}(q^2)$ obtained by LCSR are only reliable in the small positive q^2 or $q^2 < 0$ regions, instead of the physical region $q^2 > 0$. Therefore, one has to fit the form factors in the $q^2 < 0$ region by a suitable parameterization function, and extend the form factors to physical region. In this work, we use the z-series formula

[34] with single pole structure to perform the fitting, which reads as

$$\begin{aligned} F_{1,2}(q^2) = \frac{F_{1,2}(0)}{1 - \frac{q^2}{m_{\text{pole}}^2}} \left[1 + b_{1,2}(z(q^2) - z(0)) \right. \\ \left. + c_{1,2}(z(q^2) - z(0))^2 \right], \end{aligned} \quad (38)$$

where m_{pole} is the mass of the lowest baryon state that can be created by \mathcal{O}_{uq}^\dagger from the vacuum. For the $\Lambda_b \rightarrow \pi, K, D$ transitions, m_{pole} is chosen as $m_{\Lambda_b}, m_{\Xi_b} = 5.79 \text{ GeV}, m_{\Xi_{bc}} = 6.94 \text{ GeV}$ respectively, where $m_{\Xi_{bc}}$ is taken from QCD sum rules calculation [35]. The $F_{1,2}(0), b_{1,2}$ and $c_{1,2}$ in Eq. (38)

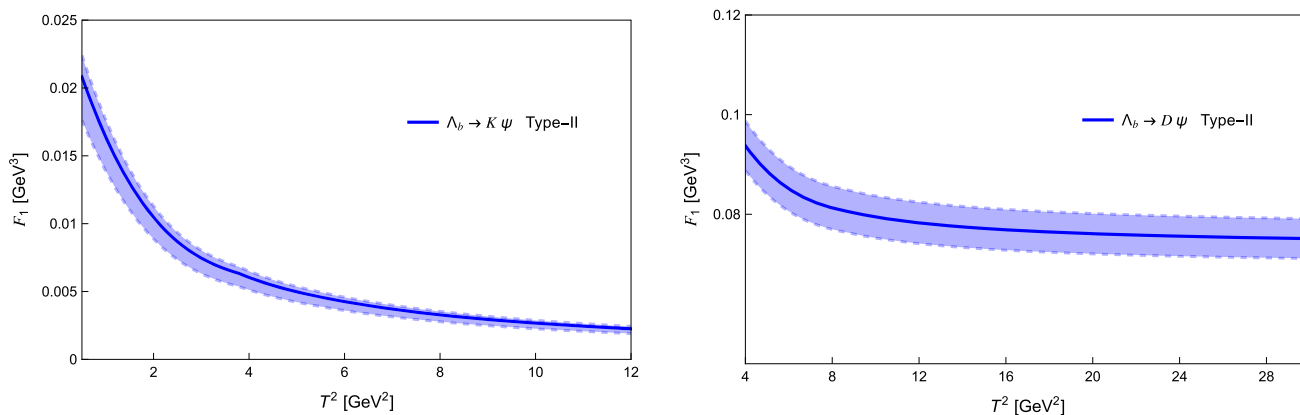


Fig. 4 The form factors F_1, F_2 as functions of T^2 in the type-II model, with $q^2 = 0$. The band width denotes the uncertainty of s_{th} : $0.6 < \lambda < 1.0$

Table 2 The maximum values of ξ in the ranges of T^2 as shown in Figs. 3 and 4

Type-I	$\Lambda_b^0 \rightarrow \pi^0$	$\Lambda_b^0 \rightarrow K^0$	$\Lambda_b^0 \rightarrow \bar{D}^0$
$F_1(0)$	$\xi < 48\%$	$\xi < 37\%$	$\xi < 35\%$
$F_2(0)$	$\xi < 36\%$	$\xi < 36\%$	$\xi < 13\%$
Type-II	–	$\Lambda_b^0 \rightarrow K^0$	$\Lambda_b^0 \rightarrow \bar{D}^0$
$F_1(0)$	–	$\xi < 10\%$	$\xi < 3\%$

are three fitting parameters, and the z function is defined as

$$z(q^2) = \frac{\sqrt{t^+ - q^2} - \sqrt{t^+ - t_0}}{\sqrt{t^+ - q^2} + \sqrt{t^+ - t_0}} \tag{39}$$

with $t^\pm = (m_{\Lambda_b} \pm m_M)^2$ and $t_0 = t^+ (1 - \sqrt{1 - t^-/t^+})$. The fitting results of $F_{1,2}(0), b_{1,2}$ and $c_{1,2}$ are listed in Table 3, while the form factors extended to the physical region are shown in Figs. 5 and 6 for the type I and II models, respectively.

With the use of form factors $F_{1,2}$ obtained above, we can calculate the decay widths of $\Lambda_b \rightarrow M\psi$ decays. The decay width formula reads as

$$\Gamma[\Lambda_b \rightarrow M\psi] = \frac{G_{(uq)}^2 |\mathbf{q}|}{8m_{\Lambda_b}^2 (2\pi)^5} \left[(m_{\Lambda_b}^2 + m_\psi^2 - m_M^2) \left(F_1^2(m_\psi^2) + \frac{m_\psi^2}{m_{\Lambda_b}^2} F_2^2(m_\psi^2) \right) + 4m_\psi^2 F_1(m_\psi^2) F_2(m_\psi^2) \right], \tag{40}$$

which is a function of the dark baryon mass m_ψ . $|\mathbf{q}|$ is the 3-momentum magnitude of the dark baryon in the center of

mass frame:

$$|\mathbf{q}| = \frac{1}{2m_{\Lambda_b}} \sqrt{(m_{\Lambda_b}^2 - (m_\psi + m_M)^2)(m_{\Lambda_b}^2 - (m_\psi - m_M)^2)}. \tag{41}$$

The upper limits of the unknown coupling constants $G_{(uq)}$ have been determined in Ref. [16] through a study of B meson semi-inclusive decays into baryons and a dark baryon, which read as

$$\begin{aligned} \text{Type I : } & G_{ud}^2 < (1.8 \pm 0.35) \times 10^{-14} \text{GeV}^{-4}, \\ & G_{us}^2 < (3.75 \pm 0.74) \times 10^{-14} \text{GeV}^{-4}, \\ & G_{cd}^2 < (1.06 \pm 0.21) \times 10^{-12} \text{GeV}^{-4}, \\ & G_{cs}^2 < (1.63 \pm 0.33) \times 10^{-12} \text{GeV}^{-4}; \\ \text{Type II : } & G_{us}^2 < (1.07 \pm 0.21) \times 10^{-11} \text{GeV}^{-4}, \\ & G_{cs}^2 < (3.62 \pm 0.72) \times 10^{-10} \text{GeV}^{-4}. \end{aligned} \tag{42}$$

Here we take $G_{(uq)}$ as their upper limit values to calculate the decay width. Accordingly, the upper limits of branching fractions for $\Lambda_b \rightarrow M\psi$ as functions of m_ψ are shown in Figs. 7 and 8 in the type I and II models, respectively. The blue and red bands denote the uncertainties from the Borel parameter and the $G_{(uq)}$ from Eq. (42).

In Sect. 4, a SU(3) analysis is performed to predict the amplitudes of all the anti-triplet bottom baryon decays into a meson and dark baryon. In the type-I model, using Eq. (34) one can further determine $\xi_{K/\pi}$ by the ratio of branching fractions:

$$\frac{1}{2}(1 + \xi_{K/\pi})^2 \lambda_{s/d}^2 = \frac{\mathcal{B}(\Lambda_b^0 \rightarrow K^0\psi)}{\mathcal{B}(\Lambda_b^0 \rightarrow \pi^0\psi)}, \tag{43}$$

if the phase space volume of $\Lambda_b^0 \rightarrow K^0\psi$ is assumed to be the same as that of $\Lambda_b^0 \rightarrow \pi^0\psi$. The $\xi_{K/\pi}$ as a function of m_ψ is shown in the left diagram of Fig. 9, where the range of

Table 3 Fitting parameters of the $F_{1,2}$ for $\Lambda_b \rightarrow \pi, K, D$ transitions in the Type-I and II models

Type-I	$F_1(0)$	b_1	c_1	$F_2(0)$	b_2	c_2
$\Lambda_b^0 \rightarrow \pi^0$	-0.02 ± 0.005	-15.77	16.41	0.07 ± 0.014	-3.81	4.43
$\Lambda_b^0 \rightarrow K^0$	0.04 ± 0.006	-5.74	12.34	-0.04 ± 0.006	-5.88	13.32
$\Lambda_b^0 \rightarrow \bar{D}^0$	0.01 ± 0.001	26.79	-35.06	0.06 ± 0.003	-4.0	11.89
Type-II	$F_1(0)$	b_1	c_1	$F_2(0)$	b_2	c_2
$\Lambda_b^0 \rightarrow K^0$	0.003 ± 0.001	6.21	-5.76	—	—	—
$\Lambda_b^0 \rightarrow \bar{D}^0$	0.07 ± 0.0	-1.01	-17.6	—	—	—

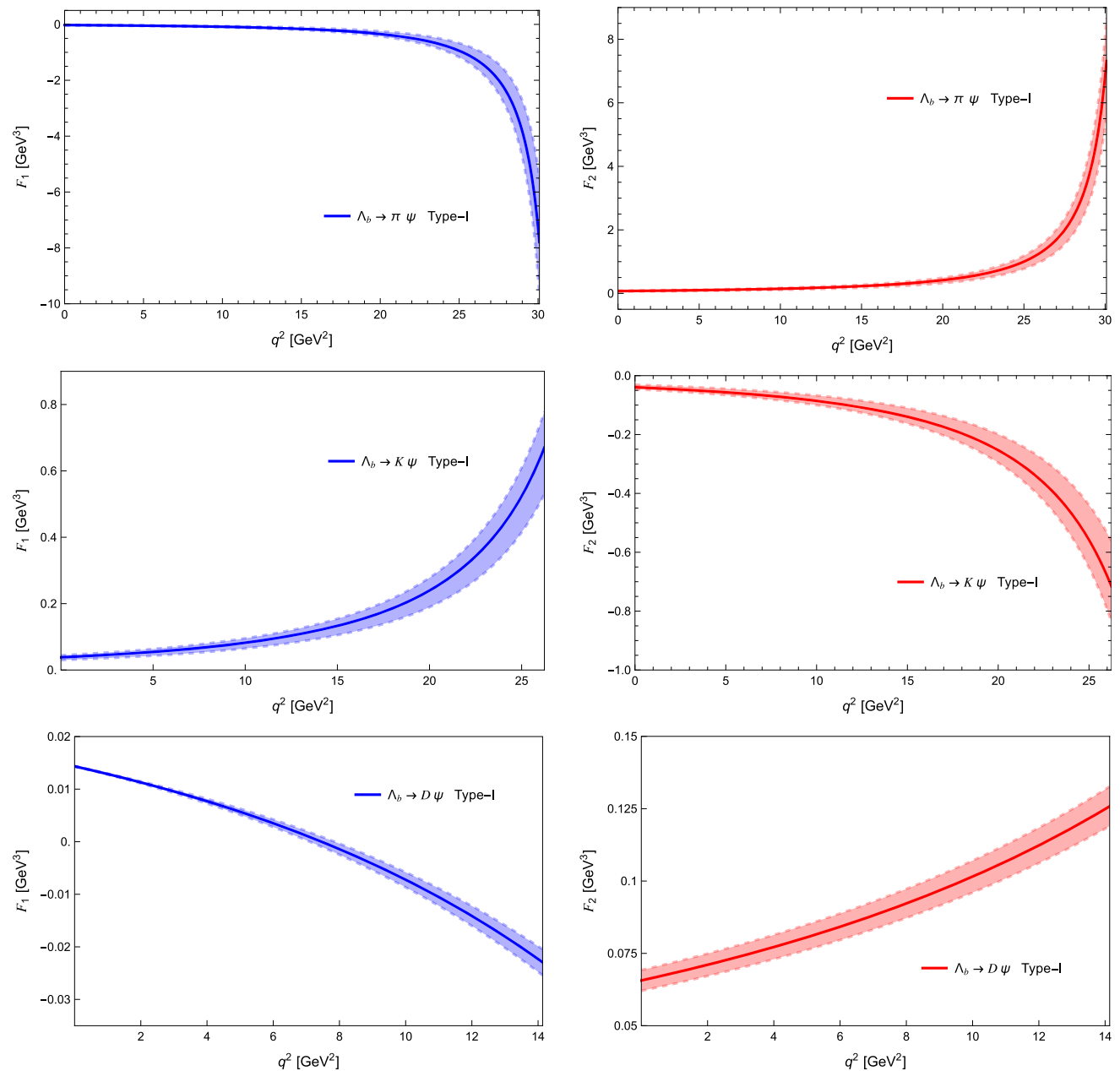


Fig. 5 The form factors F_1, F_2 as functions of q^2 in the type-I model. The band width denotes the combined uncertainties of the Borel parameter and s_{th} : $0.6 < \lambda < 1.0$

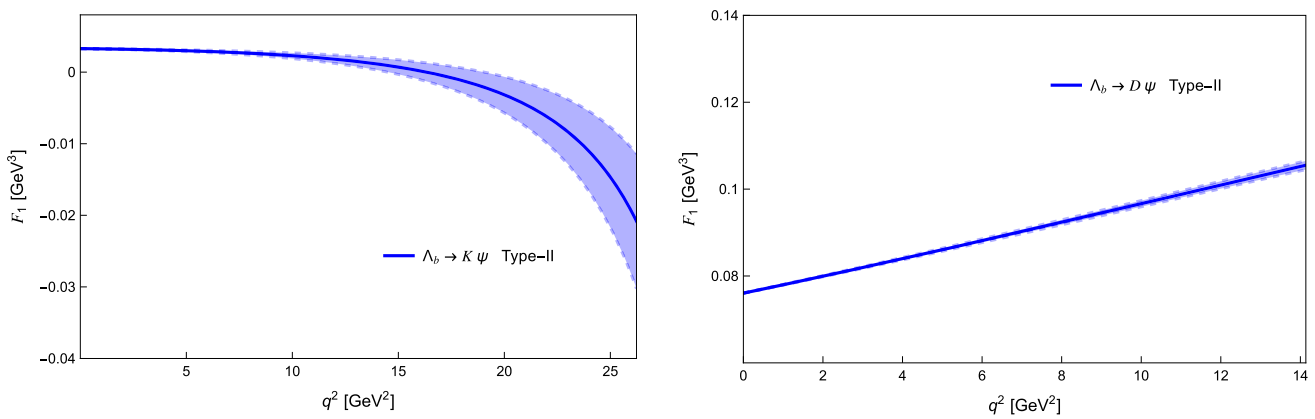


Fig. 6 The form factors F_1, F_2 as functions of q^2 in the type-II model. The band width denotes the combined uncertainties of the Borel parameter and s_{th} : $0.6 < \lambda < 1.0$

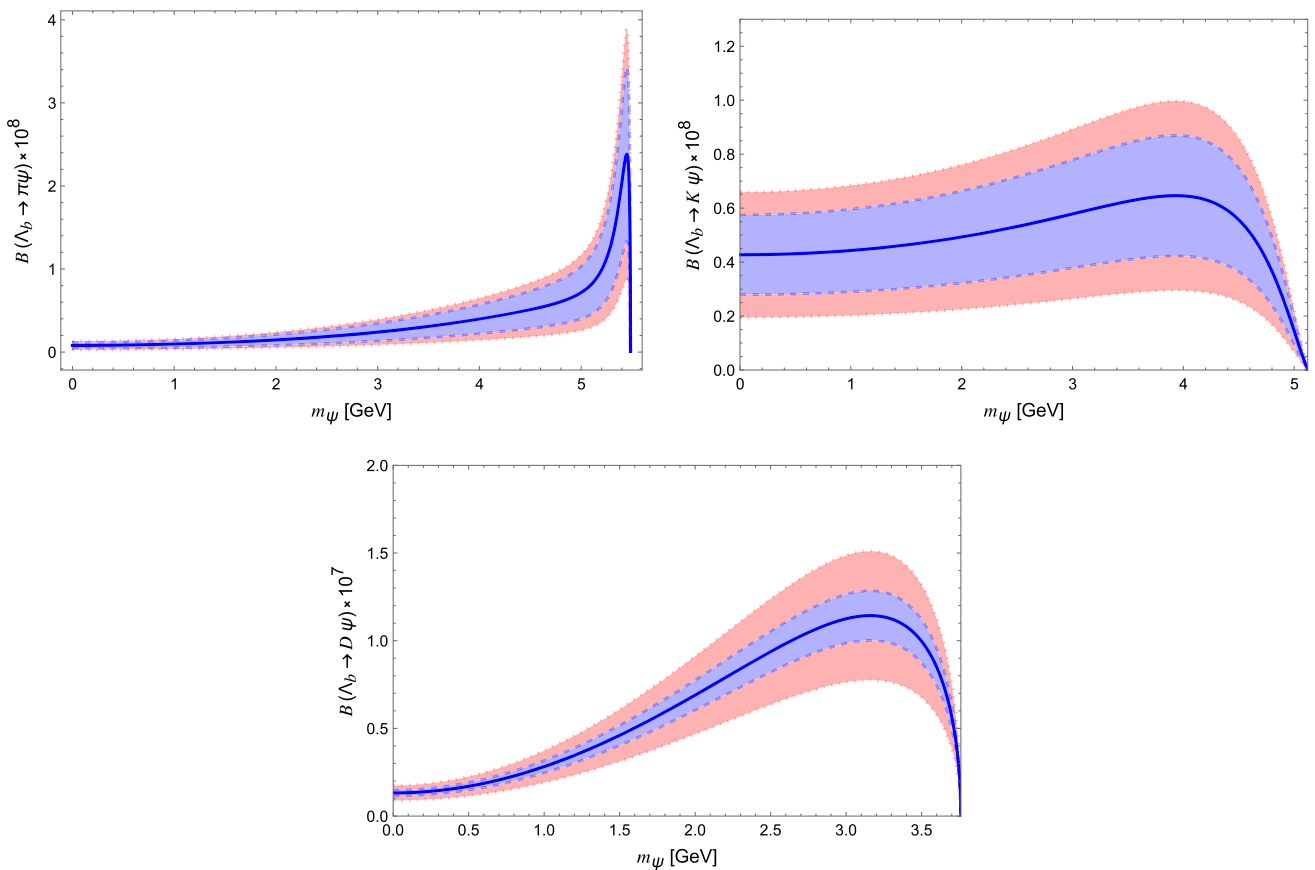


Fig. 7 The upper limits of branching fractions for $\Lambda_b \rightarrow M\psi$ as functions of m_ψ in the type-I model. The blue and red bands denote the uncertainties from the Borel parameter and the $G_{(uq)}$ from Eq. (42)

m_ψ is chosen as $0 < m_\psi < (m_{\Lambda_b} - m_K)$ and G_{ud}, G_{us} are taken as the center values in Eq. (42).

Now the branching fractions of all the decay channels listed in Table 1 can be expressed in the units of $\mathcal{B}(\Lambda_b^0 \rightarrow \pi^0 \psi)$ and $\mathcal{B}(\Lambda_b^0 \rightarrow K^0 \psi)$ for the type-I and II models respectively, which are shown in Table 4. Particularly, the branching fraction of the charged decay $\Xi_b^- \rightarrow K^- \psi$ in the

type-I model is shown in the right diagram of Fig. 9. The branching fraction of $\Xi_b^- \rightarrow \pi^- \psi$ has the same shape as $\Xi_b^- \rightarrow K^- \psi$ but a factor $\lambda_{s/d}^2$ should be timed on it.

The branching fractions of the charged decays in the type-II model are simply proportional to $\mathcal{B}(\Lambda_b^0 \rightarrow K^0 \psi)$ so we do not plot them here.

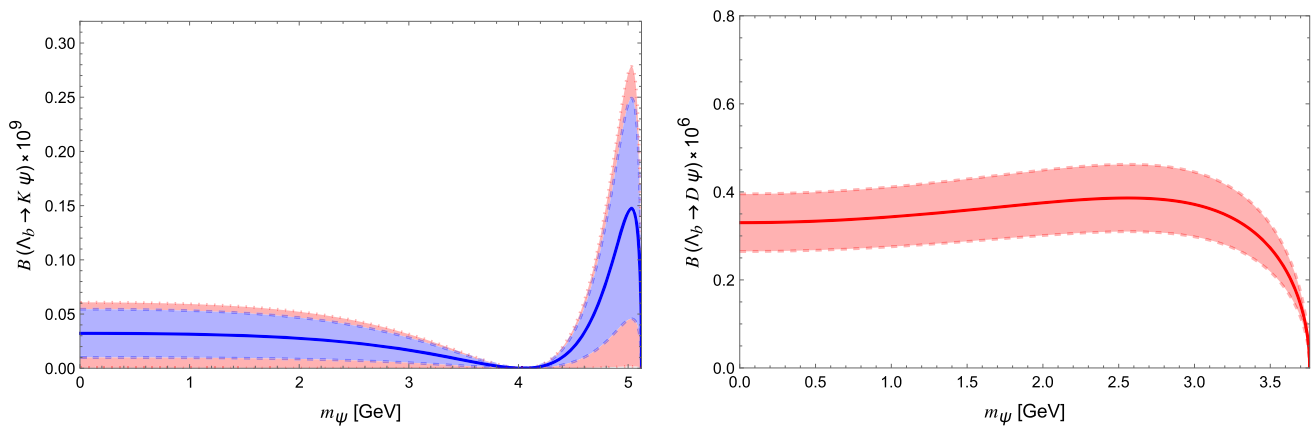


Fig. 8 The upper limits of branching fractions for $\Lambda_b \rightarrow M\psi$ as functions of m_ψ in the type-II model. The blue and red bands denote the uncertainties from the Borel parameter and the $G_{(uq)}$ from Eq. (42)

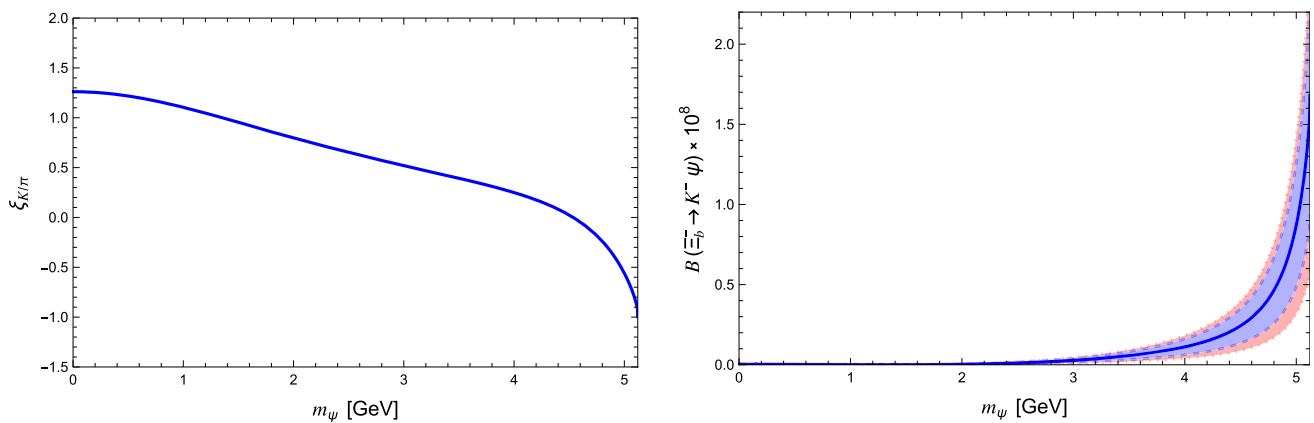


Fig. 9 The $\xi_{K/\pi}$ as a function of m_ψ from Eq. (43), where the range of m_ψ is chosen as $0 < m_\psi < (m_{\Lambda_b} - m_K)$ (left). The branching fractions of $\Xi_b^- \rightarrow K^- \psi$ as functions of m_ψ in the type-I model (right). The blue and red bands denote the uncertainties from the Borel parameter and the $G_{(ud)}$ from Eq. (42)

Table 4 The amplitudes of all the anti-triplet bottom baryon decays into a light meson and dark baryon are expressed in the units of $\mathcal{B}(\Lambda_b^0 \rightarrow \pi^0 \psi)$ and $\mathcal{B}(\Lambda_b^0 \rightarrow K^0 \psi)$ for the type-I and II models, respectively

Channel	Type-I Br.	Channel	Type-I Br.
$\Lambda_b^0 \rightarrow \pi^0 \psi$	1	$\Lambda_b^0 \rightarrow K^0 \psi$	$\frac{1}{2}(1 + \xi_{K/\pi})^2 \lambda_{s/d}^2$
$\Xi_b^0 \rightarrow \bar{K}^0 \psi$	$\frac{1}{2}(1 + \xi_{K/\pi})^2$	$\Xi_b^0 \rightarrow \pi^0 \psi$	$\frac{1}{4}(1 - \xi_{K/\pi})^2 \lambda_{s/d}^2$
$\Xi_b^- \rightarrow K^- \psi$	$\frac{1}{2}(1 - \xi_{K/\pi})^2$	$\Xi_b^- \rightarrow \pi^- \psi$	$\frac{1}{2}(1 - \xi_{K/\pi})^2 \lambda_{s/d}^2$
$\Lambda_b^0 \rightarrow \eta \psi$	$\frac{1}{3} \xi_{K/\pi}^2$	$\Xi_b^0 \rightarrow \eta \psi$	$\frac{1}{12}(1 - 3\xi_{K/\pi})^2 \lambda_{s/d}^2$
Channel	Type-II Br.	Channel	Type-II Br.
$\Lambda_b^0 \rightarrow \pi^0 \psi$	0	$\Lambda_b^0 \rightarrow K^0 \psi$	1
$\Xi_b^0 \rightarrow \bar{K}^0 \psi$	$\lambda_{s/d}^{-2}$	$\Xi_b^0 \rightarrow \pi^0 \psi$	1/2
$\Xi_b^- \rightarrow K^- \psi$	$\lambda_{s/d}^{-2}$	$\Xi_b^- \rightarrow \pi^- \psi$	1
$\Lambda_b^0 \rightarrow \eta \psi$	$\frac{2}{3} \lambda_{s/d}^{-2}$	$\Xi_b^0 \rightarrow \eta \psi$	1/6

6 Conclusion

In this work, we have studied the decays of Heavy baryon into a pseudoscalar meson and a dark baryon using the recently developed *B*-Mesogenesis scenario, where the two types of effective Lagrangians proposed by the scenario are both considered. The decay amplitudes of Λ_b^0 have been calculated by LCSR using its light-cone distribution amplitudes. The decay amplitudes of $\Xi_b^{0,\pm}$ has been related with those of Λ_b^0 through a flavor SU(3) analysis. In the numerical calculation, the uncertainties of threshold parameter and the Borel parameter are both considered. The values of effective coupling constants in the *B*-Mesogenesis are taken as their upper limits that obtained from our previous study on the inclusive decay. The upper limits of the decay branching fractions of $\Lambda_b^0, \Xi_b^{0,\pm} \rightarrow M\psi$ are presented as functions of the dark baryon mass, which will be tested by future experimental detections.

Funding The work of Y.J. Shi is supported by Natural Science Foundation of China under Grant No. 12305103, and Opening Foundation of Shanghai Key Laboratory of Particle Physics and Cosmology under Grant No. 22DZ2229013-2. The work of Y. Xing is supported by National Science Foundation of China under Grant No. 12005294. The work of Z.P. Xing is supported by China Postdoctoral Science Foundation under Grant No. 2022M72210.

Data Availability Statement This manuscript has no associated data or the data will not be deposited. [Authors' comment: This is a theoretical study and no experimental data.]

Code availability The manuscript has no associated code/software. [Authors' comment: Not applicable.]

Open Access This article is licensed under a Creative Commons Attribution 4.0 International License, which permits use, sharing, adaptation, distribution and reproduction in any medium or format, as long as you give appropriate credit to the original author(s) and the source, provide a link to the Creative Commons licence, and indicate if changes were made. The images or other third party material in this article are included in the article's Creative Commons licence, unless indicated otherwise in a credit line to the material. If material is not included in the article's Creative Commons licence and your intended use is not permitted by statutory regulation or exceeds the permitted use, you will need to obtain permission directly from the copyright holder. To view a copy of this licence, visit <http://creativecommons.org/licenses/by/4.0/>.
Funded by SCOAP³.

Appendix A Analytical results in the type-I model

In this appendix, we present the analytical results of the quark-gluon level calculation for the correlation function defined in Eq. (7). In the type-I model, the twist-3s contribution to the correlation function for the $\Lambda_b \rightarrow \pi$ decay is

$$\begin{aligned} \mathcal{B}\{\Pi_{\Lambda_b \rightarrow \pi}^{QCD(3s)}\}(T, q) &= \frac{i}{4\sqrt{2}} f_{\Lambda_b}^{(1)} \int_0^{2s_0^{\Lambda_b}} d\omega \\ &\times \int_0^1 du \theta(\Sigma - s_m)\theta(s_{th} - \Sigma) e^{-\Sigma/T^2} \\ &\times \psi_{3s}(\omega, u) P_R \left[m_{\Lambda_b} \omega \not{q} - \frac{m_{\Lambda_b} \omega}{m_{\Lambda_b} - u\omega} q^2 \right] \\ &+ \frac{i}{4\sqrt{2}} f_{\Lambda_b}^{(1)} \int_0^{2s_0^{\Lambda_b}} d\omega \int_0^1 du \theta(\bar{\Sigma} - s_m)\theta(s_{th} - \bar{\Sigma}) e^{-\bar{\Sigma}/T^2} \\ &\times \psi_{3s}(\omega, u) P_R \left[(\bar{u}\omega(2q \cdot v) - 2p \cdot q - q^2) \frac{\omega m_{\Lambda_b}}{m_{\Lambda_b} - \bar{u}\omega} \right. \\ &\left. + m_{\Lambda_b} \omega \not{q} \right] u_{\Lambda_b}(v), \end{aligned} \tag{A.1}$$

where $\Sigma = \Sigma_c|_{m_c=0}$ and $\bar{\Sigma} = \Sigma|_{u \rightarrow \bar{u}}$. The twist-3 σ contributions are

$$\begin{aligned} \mathcal{B}\{\Pi_{\Lambda_b \rightarrow \pi}^{QCD(3\sigma)}\}(p, q) &= -\frac{i}{4\sqrt{2}} f_{\Lambda_b}^{(1)} \int_0^{2s_0^{\Lambda_b}} d\omega \\ &\times \int_0^1 du \theta(\Sigma - s_m)\theta(s_{th} - \Sigma) e^{-\Sigma/T^2} \\ &\times \psi_{3s}(\omega, u) P_R \left[m_{\Lambda_b} \omega \not{q} - \frac{m_{\Lambda_b} \omega}{m_{\Lambda_b} - u\omega} q^2 \right] u_{\Lambda_b}(v) \\ &- \frac{i}{4\sqrt{2}} f_{\Lambda_b}^{(1)} \int_0^{2s_0^{\Lambda_b}} d\omega \int_0^1 du \theta(\bar{\Sigma} - s_m)\theta(s_{th} - \bar{\Sigma}) e^{-\bar{\Sigma}/T^2} \\ &\times \psi_{3\sigma}(\omega, u) P_R \left[(\bar{u}\omega(2q \cdot v) - 2p \cdot q - q^2) \frac{\omega m_{\Lambda_b}}{m_{\Lambda_b} - \bar{u}\omega} \right. \\ &\left. + m_{\Lambda_b} \omega \not{q} \right] u_{\Lambda_b}(v) \\ &- \frac{i}{2\sqrt{2}} f_{\Lambda_b}^{(1)} \frac{\partial}{\partial M^2} \int_0^{2s_0^{\Lambda_b}} d\omega \int_0^1 du \bar{\psi}_{3\sigma}(\omega, u) e^{-(\Sigma+M^2)/T^2} \\ &\times \theta((\Sigma + M^2) - s_m)\theta(s_{th} - (\Sigma + M^2)) \left(\frac{m_{\Lambda_b}}{m_{\Lambda_b} - u\omega} \right)^2 \\ &\times P_R [A(p^2, q^2) + B(p^2, q^2)\not{q}] u_{\Lambda_b}(v) \Big|_{M^2=0, p^2=\Sigma+M^2} \\ &+ \frac{i}{\sqrt{2}} f_{\Lambda_b}^{(1)} \frac{\partial}{\partial M^2} \int_0^{2s_0^{\Lambda_b}} d\omega \int_0^1 du \bar{\psi}_{3\sigma}(\omega, u) e^{-(\bar{\Sigma}+M^2)/T^2} \\ &\times \theta((\bar{\Sigma} + M^2) - s_m)\theta(s_{th} - (\bar{\Sigma} + M^2)) \left(\frac{m_{\Lambda_b}}{m_{\Lambda_b} - \bar{u}\omega} \right)^2 \\ &\times (p \cdot q - \bar{u}\omega v \cdot q) P_R (m_{\Lambda_b} - \bar{u}\omega - \not{q}) u_{\Lambda_b}(v) \\ &\Big|_{M^2=0, p^2=\bar{\Sigma}+M^2}, \end{aligned} \tag{A.2}$$

The twist-3s and twist-3 σ contributions to the correlation function for the $\Lambda_b \rightarrow K$ decay are

$$\begin{aligned}
 \mathcal{B}\{\Pi_{\Lambda_b \rightarrow K}^{QCD(3s)}\}(T, q) &= -\frac{i}{4} f_{\Lambda_b}^{(1)} \int_0^{2s_0^{\Lambda_b}} d\omega \\
 &\times \int_0^1 du \theta(\bar{\Sigma} - s_m) \theta(s_{th} - \bar{\Sigma}) e^{-\bar{\Sigma}/T^2} \\
 &\times \psi_{3s}(\omega, u) P_R \left[(\bar{u}\omega(2q \cdot v) - 2p \cdot q - q^2) \frac{\omega m_{\Lambda_b}}{m_{\Lambda_b} - \bar{u}\omega} \right. \\
 &\left. + m_{\Lambda_b} \omega \not{q} \right] u_{\Lambda_b}(v), \\
 \mathcal{B}\{\Pi_{\Lambda_b \rightarrow K}^{QCD(3\sigma)}\}(p, q) &= \frac{i}{4} f_{\Lambda_b}^{(1)} \int_0^{2s_0^{\Lambda_b}} d\omega \\
 &\times \int_0^1 du \theta(\bar{\Sigma} - s_m) \theta(s_{th} - \bar{\Sigma}) e^{-\bar{\Sigma}/T^2} \\
 &\times \psi_{3\sigma}(\omega, u) P_R \left[(\bar{u}\omega(2q \cdot v) - 2p \cdot q - q^2) \frac{\omega m_{\Lambda_b}}{m_{\Lambda_b} - \bar{u}\omega} \right. \\
 &\left. + m_{\Lambda_b} \omega \not{q} \right] u_{\Lambda_b}(v) \\
 &- i f_{\Lambda_b}^{(1)} \frac{\partial}{\partial M^2} \int_0^{2s_0^{\Lambda_b}} d\omega \int_0^1 du \bar{\psi}_{3\sigma}(\omega, u) e^{-(\bar{\Sigma}+M^2)/T^2} \\
 &\times \theta((\bar{\Sigma} + M^2) - s_m) \theta(s_{th} - (\bar{\Sigma} + M^2)) \left(\frac{m_{\Lambda_b}}{m_{\Lambda_b} - \bar{u}\omega} \right)^2 \\
 &\times (p \cdot q - \bar{u}\omega v \cdot q) P_R (m_{\Lambda_b} - \bar{u}\omega - \not{q}) u_{\Lambda_b}(v) \\
 &\times \Big|_{M^2=0, p^2=\bar{\Sigma}+M^2}. \tag{A. 3}
 \end{aligned}$$

The twist-2, 4 contributions to the correlation function for the $\Lambda_b \rightarrow \pi, K$ decays vanishes in the chiral limit $m_u = m_d = 0$.

Appendix B Analytical results in the type-II model

In the type-II model, the $\Lambda_b \rightarrow \pi$ decay is forbidden in the flavor SU(3) limit. The twist-3s and twist-3 σ contributions to the correlation function for the $\Lambda_b \rightarrow K$ decay are

$$\begin{aligned}
 \mathcal{B}\{\Pi_{\Lambda_b \rightarrow K}^{QCD(3s)}\}(T, q) &= -\frac{i}{2} f_{\Lambda_b}^{(1)} \int_0^{2s_0^{\Lambda_b}} d\omega \\
 &\times \int_0^1 du \theta(\bar{\Sigma} - s_m) \theta(s_{th} - \bar{\Sigma}) e^{-\bar{\Sigma}/T^2} \\
 &\times \psi_{3s}(\omega, u) \frac{\omega m_{\Lambda_b}}{m_{\Lambda_b} - \bar{u}\omega} P_R [\bar{u}\omega v \cdot q - p \cdot q] u_{\Lambda_b}(v), \\
 \mathcal{B}\{\Pi_{\Lambda_b \rightarrow K}^{QCD(3\sigma)}\}(p, q) &= \frac{i}{2} f_{\Lambda_b}^{(1)} \int_0^{2s_0^{\Lambda_b}} d\omega \\
 &\times \int_0^1 du \theta(\bar{\Sigma} - s_m) \theta(s_{th} - \bar{\Sigma}) e^{-\bar{\Sigma}/T^2} \\
 &\times \psi_{3\sigma}(\omega, u) \frac{\omega m_{\Lambda_b}}{m_{\Lambda_b} - \bar{u}\omega} P_R [\bar{u}\omega v \cdot q - p \cdot q] u_{\Lambda_b}(v) \\
 &- 2i f_{\Lambda_b}^{(1)} \frac{\partial}{\partial M^2} \int_0^{2s_0^{\Lambda_b}} d\omega \int_0^1 du \bar{\psi}_{3\sigma}(\omega, u) e^{-(\bar{\Sigma}+M^2)/T^2}
 \end{aligned}$$

$$\begin{aligned}
 &\times \theta((\bar{\Sigma} + M^2) - s_m) \theta(s_{th} - (\bar{\Sigma} + M^2)) \left(\frac{m_{\Lambda_b}}{m_{\Lambda_b} - \bar{u}\omega} \right)^2 \\
 &\times (v \cdot p - \bar{u}\omega)(p \cdot q - \bar{u}\omega v \cdot q) P_R u_{\Lambda_b}(v) \Big|_{M^2=0, p^2=\bar{\Sigma}+M^2}. \tag{B. 1}
 \end{aligned}$$

The twist-2+4 contributions to the correlation function for the $\Lambda_b \rightarrow D$ decay are

$$\begin{aligned}
 \mathcal{B}\{\Pi_{\Lambda_b \rightarrow D}^{QCD(2+4)}\}(p, q) &= \frac{i}{2} m_c f_{\Lambda_b}^{(2)} \int_0^{2s_0^{\Lambda_b}} d\omega \\
 &\times \int_0^1 du \theta(\Sigma_c - s_m) \theta(s_{th} - \Sigma_c) e^{-\Sigma_c/T^2} \\
 &\times \psi_2(\omega, u) \frac{\omega m_{\Lambda_b}}{m_{\Lambda_b} - \bar{u}\omega} (v \cdot q) P_R u_{\Lambda_b}(v) \\
 &+ \frac{i}{2} m_c f_{\Lambda_b}^{(2)} \frac{\partial}{\partial M^2} \int_0^{2s_0^{\Lambda_b}} d\omega \\
 &\times \int_0^1 du (\bar{\psi}_2 - \bar{\psi}_4)(\omega, u) e^{-(\Sigma_c+M^2)/T^2} \\
 &\times \theta((\Sigma_c + M^2) - s_m) \theta(s_{th} - (\Sigma_c + M^2)) \left(\frac{m_{\Lambda_b}}{m_{\Lambda_b} - \bar{u}\omega} \right)^2 \\
 &\times (p \cdot q - u\omega v \cdot q) P_R u_{\Lambda_b}(v) \Big|_{M^2=0, p^2=\Sigma_c+M^2}. \tag{B. 2}
 \end{aligned}$$

The twist-3 contributions to the correlation function for the $\Lambda_b \rightarrow D$ decay are

$$\begin{aligned}
 \mathcal{B}\{\Pi_{\Lambda_b \rightarrow D}^{QCD(3s)}\}(p, q) &= -i f_{\Lambda_b}^{(1)} \int_0^{2s_0^{\Lambda_b}} d\omega \\
 &\times \int_0^1 du \theta(\Sigma_c - s_m) \theta(s_{th} - \Sigma_c) e^{-\Sigma_c/T^2} \\
 &\times (\psi_{3s} + \psi_{3\sigma})(\omega, u) \frac{\omega m_{\Lambda_b}}{m_{\Lambda_b} - \bar{u}\omega} (u\omega v \cdot q - p \cdot q) P_R u_{\Lambda_b}(v) \\
 &+ 2i f_{\Lambda_b}^{(1)} \frac{\partial}{\partial M^2} \int_0^{2s_0^{\Lambda_b}} d\omega \\
 &\times \int_0^1 du \bar{\psi}_{3\sigma}(\omega, u) e^{-(\Sigma_c+M^2)/T^2} \\
 &\times \theta((\Sigma_c + M^2) - s_m) \theta(s_{th} - (\Sigma_c + M^2)) \left(\frac{m_{\Lambda_b}}{m_{\Lambda_b} - \bar{u}\omega} \right)^2 \\
 &\times (v \cdot p - u\omega)(p \cdot q - u\omega v \cdot q) P_R u_{\Lambda_b}(v) \\
 &\times \Big|_{M^2=0, p^2=\Sigma_c+M^2}. \tag{B. 3}
 \end{aligned}$$

References

1. A.D. Sakharov, Violation of CP invariance, C asymmetry, and baryon asymmetry of the universe. *Pisma Zh. Eksp. Teor. Fiz.* **5**, 32 (1967). <https://doi.org/10.1070/PU1991v034n05ABEH002497>

2. G. Elor, M. Escudero, A. Nelson, Baryogenesis and dark matter from B mesons. Phys. Rev. D **99**(3), 035031 (2019). <https://doi.org/10.1103/PhysRevD.99.035031>. arXiv:1810.00880 [hep-ph]
3. G. Alonso-Álvarez, G. Elor, M. Escudero, Collider signals of baryogenesis and dark matter from B mesons: a roadmap to discovery. Phys. Rev. D **104**3, 035028 (2021). <https://doi.org/10.1103/PhysRevD.104.035028>. arXiv:2101.02706 [hep-ph]
4. F. Elahi, G. Elor, R. McGehee, Charged B mesogenesis. Phys. Rev. D **105**5, 055024 (2022). <https://doi.org/10.1103/PhysRevD.105.055024>. arXiv:2109.09751 [hep-ph]
5. A.E. Nelson, H. Xiao, Phys. Rev. D **100**(7), 075002 (2019). <https://doi.org/10.1103/PhysRevD.100.075002>. arXiv:1901.08141 [hep-ph]
6. G. Alonso-Álvarez, G. Elor, A.E. Nelson, H. Xiao, JHEP **03**, 046 (2020). [https://doi.org/10.1007/JHEP03\(2020\)046](https://doi.org/10.1007/JHEP03(2020)046). arXiv:1907.10612 [hep-ph]
7. M. Borsato, X. Cid Vidal, Y. Tsai, C. Vázquez Sierra, J. Zurita, G. Alonso-Álvarez, A. Boyarsky, A. Brea Rodríguez, D. Buarque Franzosi, G. Cacciapaglia et al., Unleashing the full power of LHCb to probe stealth new physics. Rep. Prog. Phys. **85**(2), 024201 (2022). <https://doi.org/10.1088/1361-6633/ac4649>. arXiv:2105.12668 [hep-ph]
8. G. Alonso-Álvarez, G. Elor, M. Escudero, B. Fornal, B. Grinstein, J. Martin Camalich, Strange physics of dark baryons. Phys. Rev. D **105**11, 115005 (2022). <https://doi.org/10.1103/PhysRevD.105.115005>. arXiv:2111.12712 [hep-ph]
9. E. Goudzovski, D. Redigolo, K. Tobioka, J. Zupan, G. Alonso-Álvarez, D.S.M. Alves, S. Bansal, M. Bauer, J. Brod, V. Chobanova et al., New physics searches at kaon and hyperon factories. Rep. Prog. Phys. **86**1, 016201 (2023). <https://doi.org/10.1088/1361-6633/ac9cee>. arXiv:2201.07805 [hep-ph]
10. C. Hadjivasiliou et al. [Belle], Search for B^0 meson decays into Λ and missing energy with a hadronic tagging method at Belle. Phys. Rev. D **105**5, L051101 (2022). <https://doi.org/10.1103/PhysRevD.105.L051101>. arXiv:2110.14086 [hep-ex]
11. A.B. Rodríguez, V. Chobanova, X. CidVidal, S.L. Soliño, D.M. Santos, T. Mombächer, C. Prouvé, E.X.R. Fernández, C. Vázquez Sierra, Prospects on searches for baryonic Dark Matter produced in b -hadron decays at LHCb. Eur. Phys. J. C **81**11, 964 (2021). <https://doi.org/10.1140/epjc/s10052-021-09762-w>. arXiv:2106.12870 [hep-ph]
12. A. Khodjamirian, M. Wald, B -meson decay into a proton and dark antibaryon from QCD light-cone sum rules. Phys. Lett. B **834**, 137434 (2022). <https://doi.org/10.1016/j.physletb.2022.137434>. arXiv:2206.11601 [hep-ph]
13. A. Boushmeliev, M. Wald, Higher twist corrections to B -meson decays into a proton and dark antibaryon from QCD light-cone sum rules. arXiv:2311.13482 [hep-ph]
14. G. Elor, A.W.M. Guerrero, Branching fractions of B meson decays in mesogenesis. JHEP **02**, 100 (2023). [https://doi.org/10.1007/JHEP02\(2023\)100](https://doi.org/10.1007/JHEP02(2023)100). arXiv:2211.10553 [hep-ph]
15. C.O. Dib, J.C. Helo, V.E. Lyubovitskij, N.A. Neill, A. Soffer, Z.S. Wang, Probing R-parity violation in B -meson decays to a baryon and a light neutralino. JHEP **02**, 224 (2023). [https://doi.org/10.1007/JHEP02\(2023\)224](https://doi.org/10.1007/JHEP02(2023)224). arXiv:2208.06421 [hep-ph]
16. Y.J. Shi, Y. Xing, Z.P. Xing, Semi-inclusive decays of B meson into a dark anti-baryon and baryons. Eur. Phys. J. C **83**8, 744 (2023). <https://doi.org/10.1140/epjc/s10052-023-11930-z>. arXiv:2305.17622 [hep-ph]
17. R. Barate et al. [ALEPH], Measurements of $\text{BR}(b \rightarrow \tau \bar{\nu}_\tau X)$ and $\text{BR}(b \rightarrow \tau \bar{\nu}_\tau D^{*\pm} X)$ and upper limits on $\text{BR}(B^- \rightarrow \tau \bar{\nu}_\tau X)$ and $\text{BR}(b \rightarrow s \nu \bar{\nu})$. Eur. Phys. J. C **19**, 213–227 (2001). <https://doi.org/10.1007/s100520100612>. arXiv:hep-ex/0010022 [hep-ex]
18. D. Buskulic et al. [ALEPH], Measurement of the $b \rightarrow \tau \bar{\nu}_\tau X$ branching ratio. Phys. Lett. B **298**, 479–491 (1993). [https://doi.org/10.1016/0370-2693\(93\)91853-F](https://doi.org/10.1016/0370-2693(93)91853-F)
19. D. Buskulic et al. [ALEPH], Measurement of the $b \rightarrow \tau \bar{\nu}_\tau X$ branching ratio and an upper limit on $B \rightarrow \tau \bar{\nu}_\tau \nu$. Phys. Lett. B **343**, 444–452 (1995). [https://doi.org/10.1016/0370-2693\(94\)01584-Y](https://doi.org/10.1016/0370-2693(94)01584-Y)
20. L.L. Chau, H.Y. Cheng, Quark diagram analysis of two-body charm decays. Phys. Rev. Lett. **56**, 1655–1658 (1986). <https://doi.org/10.1103/PhysRevLett.56.1655>
21. L.L. Chau, H.Y. Cheng, Analysis of exclusive two-body decays of charm mesons using the quark diagram scheme. Phys. Rev. D **36**, 137 (1987). <https://doi.org/10.1103/PhysRevD.36.137>
22. L.L. Chau, H.Y. Cheng, W.K. Sze, H. Yao, B. Tseng, Charmless nonleptonic rare decays of B mesons. Phys. Rev. D **43**, 2176–2192 (1991). <https://doi.org/10.1103/PhysRevD.43.2176> [Erratum: Phys. Rev. D **58**, 019902 (1998)]
23. M. Gronau, O.F. Hernandez, D. London, J.L. Rosner, Decays of B mesons to two light pseudoscalars. Phys. Rev. D **50**, 4529–4543 (1994). <https://doi.org/10.1103/PhysRevD.50.4529>. arXiv:hep-ph/9404283 [hep-ph]
24. S.H. Zhou, Q.A. Zhang, W.R. Lyu, C.D. Lü, Analysis of charmless two-body B decays in factorization assisted topological amplitude approach. Eur. Phys. J. C **77**2, 125 (2017). <https://doi.org/10.1140/epjc/s10052-017-4685-0>. arXiv:1608.02819 [hep-ph]
25. S. Müller, U. Nierste, S. Schacht, Topological amplitudes in D decays to two pseudoscalars: a global analysis with linear $SU(3)_F$ breaking. Phys. Rev. D **92**1, 014004 (2015). <https://doi.org/10.1103/PhysRevD.92.014004>. arXiv:1503.06759 [hep-ph]
26. Y.J. Shi, W. Wang, Y. Xing, J. Xu, Weak decays of doubly heavy baryons: multi-body decay channels. Eur. Phys. J. C **78**1, 56 (2018). <https://doi.org/10.1140/epjc/s10052-018-5532-7>. arXiv:1712.03830 [hep-ph]
27. D. Zeppenfeld, $SU(3)$ relations for B meson decays. Z. Phys. C **8**, 77 (1981). <https://doi.org/10.1007/BF01429835>
28. X.G. He, W. Wang, Flavor $SU(3)$ topological diagram and irreducible representation amplitudes for heavy meson charmless hadronic decays: mismatch and equivalence. Chin. Phys. C **42**10, 103108 (2018). <https://doi.org/10.1088/1674-1137/42/10/103108>. arXiv:1803.04227 [hep-ph]
29. X.G. He, Y.J. Shi, W. Wang, Unification of flavor $SU(3)$ analyses of heavy hadron weak decays. Eur. Phys. J. C **80**5, 359 (2020). <https://doi.org/10.1140/epjc/s10052-020-7862-5>. arXiv:1811.03480 [hep-ph]
30. D. Wang, C.P. Jia, F.S. Yu, A self-consistent framework of topological amplitude and its $SU(N)$ decomposition. JHEP **21**, 126 (2020). [https://doi.org/10.1007/JHEP09\(2021\)126](https://doi.org/10.1007/JHEP09(2021)126). arXiv:2001.09460 [hep-ph]
31. P. Ball, V.M. Braun, E. Gardi, Distribution amplitudes of the lambda(b) baryon in QCD. Phys. Lett. B **665**, 197–204 (2008). <https://doi.org/10.1016/j.physletb.2008.06.004>. arXiv:0804.2424 [hep-ph]
32. H.H. Duan, Y.L. Liu, M.Q. Huang, Light-cone sum rule analysis of semileptonic decays $\Lambda_b^0 \rightarrow \Lambda_c^+ \ell^- \bar{\nu}_\ell$. Eur. Phys. J. C **82**10, 51 (2022). <https://doi.org/10.1140/epjc/s10052-022-10931-8>. arXiv:2204.00409 [hep-ph]
33. R.L. Workman et al. [Particle Data Group], Review of particle physics. PTEP **2022**, 083C01 (2022). <https://doi.org/10.1093/ptep/ptac097>
34. C. Bourrely, I. Caprini, L. Lellouch, Model-independent description of $B \rightarrow \pi l \nu$ decays and a determination of $|V_{ub}|$. Phys. Rev. D **79**, 013008 (2009). <https://doi.org/10.1103/PhysRevD.79.013008>. arXiv:0807.2722 [hep-ph] [Erratum: Phys. Rev. D **82**, 099902 (2010)]
35. X.H. Hu, Y.L. Shen, W. Wang, Z.X. Zhao, Weak decays of doubly heavy baryons: “decay constants”. Chin. Phys. C **42**12, 123102 (2018). <https://doi.org/10.1088/1674-1137/42/12/123102>. arXiv:1711.10289 [hep-ph]